



# Stress-Strain Behavior of Confined Class C Fly Ash-Based Geopolymer Concrete

Galih Syifa'ul Ummah<sup>a</sup>, Bambang Piscesa<sup>a</sup>, Yuyun Tajunnisa<sup>b\*</sup>



<sup>a</sup>Departement of Civil Engineering, Institut Teknologi Sepuluh Nopember, Surabaya 60111, Indonesia

<sup>b</sup>Departement of Civil Infrastructure Engineering, Institut Teknologi Sepuluh Nopember, Surabaya 60111, Indonesia

## Abstract

Fly ash-based geopolymer cement has recently attracted attention due to its application potential, as well as being an alternative binder with low emissions compared to conventional portland cement in concrete production. Studies intended on the mechanical properties and behaviors of structural elements produced from class C fly ash-based geopolymer concrete are important to improve the implementation. This study aimed to determine the effect of confinement on the behavior of class C fly ash-based geopolymer concrete and portland cement-based concrete. 6 specimens were made with class C fly ash-based geopolymer concrete tested under axial loading. Then, 6 specimens were made with ordinary portland cement-based concrete for comparison. The variable considered in this study is the pitch of confinement. The effect of the pitch of confinement on the enhancement strength and stress-strain of class C fly ash-based geopolymer concrete was obtained. The analytical model proposed by Richard et al. was selected to evaluate the ultimate compressive strength and ultimate compressive strain of confined geopolymer concrete in this study. The results showed that confinement reinforcement improved the strength and ductility of class C fly ash-based geopolymer concrete.

*Keywords:* Class c fly ash; Confinement; Enhancement strength; Geopolymer concrete; Stress-strain

## 1. Introduction

Portland cement concrete production increases emissions CO<sub>2</sub> that impacted on increasing the greenhouse gases effect in the atmosphere [1]. Therefore, research on the use of fly ash material in concrete production is important to produce environmentally friendly building materials. Geopolymer concrete is an alternative material that uses silica and alumina sources such as fly ash using alkali activators [2]. Fly ash (FA), produced from coal-fired power plants, which is known to significantly improve the mechanical properties and strength of geopolymer concrete (GPC), is the commonly used aluminosilicate binder. The activator commonly used for GPC production is a combination of Na<sub>2</sub>SiO<sub>3</sub> and NaOH. The activator greatly influences the polymerization process. In addition to the Sodium Silicate/Sodium Hydroxide ratio, the molarity of NaOH also influences the polymerization process. Polymerization occurs when the alkali activator dissolves Si and Al from the binder to form a N–A–S–H gel matrix. Activators using NaOH and Na<sub>2</sub>SiO<sub>3</sub> increase the reactivity of fly ash. According to studies [3], [4], the influence of NaOH molarity affects the geopolymerization process. GPC test specimens using Na<sub>2</sub>SiO<sub>3</sub> and NaOH activators showed better mechanical properties, strength, and microstructure [5].

Class C fly ash (high-calcium fly ash) has not been utilized properly due to its relatively quick-setting time characteristics and low workability, making it difficult to implement. The weaknesses of class C fly ash-based geopolymer concrete was solved by developing a dry mixing method [6]–[12]. This refers to the study [13] as a mix design calculation. Study on dry mixing geopolymer concrete by [7] includes a study of mechanical properties so that further development is needed to determine its behavior when implemented as a construction material.

Confinement is an important factor affecting concrete behavior. Strength and ductility depend on the stress-strain characteristics of concrete and affected by element confinement. The properties of confined geopolymer concrete have been studied by previous researchers [14] limited in the scope of class F fly ash-based geopolymer concrete. To obtain a general constitutive model of confined concrete, there is insufficient data base of the results of testing the mechanical properties of concrete materials, especially on geopolymer concrete. Studies on the effect of confinement on class C

fly ash-based geopolymer concrete have been scarce. Therefore, this studies experimentally and analytically the contribution of confinement to class C fly ash-based geopolymer concrete.

**2. Method**

*2.1. Material and Mix Design*

In this study, fly ash (ASTM Class C) was used as the main source material for synthesizing geopolymer binders. The fly ash was brown color, which was analyzed using X-ray fluorescence (XRF). The chemical compositions of fly ash used are shown in Table 1. Coarse aggregate was used to fabricate GPC and PCC with a nominal size of 20 mm. Locally available river sand, which complies with zone II according to SNI 2834:2000, was used as fine aggregate. The properties of coarse aggregate and fine aggregate used are shown in Table 2 and Table 3. The manufacture of geopolymer cement was conducted using dry mixing method using alkali activator in solid form [6]. The alkali activators used in this study were NaOH<sub>(s)</sub> and Na<sub>2</sub>SiO<sub>3(s)</sub>. The molarity of NaOH used was 10 M. The molarity of NaOH 10 M showed a longer setting time for class C fly ash-based geopolymer concrete, thus enhancing the workability of the concrete (Topark-Ngarm, et al., 2015). The ratio of Na<sub>2</sub>SiO<sub>3</sub> activator to NaOH (S:H) used was 1:1. Previous study [4] showed that the ratio S:H = 1 produced higher geopolymer concrete strength.

Table 1. Chemical Composition of Fly Ash

Chemical Composition (%)									
SiO <sub>2</sub>	Al <sub>2</sub> O <sub>3</sub>	Fe <sub>2</sub> O <sub>3</sub>	CaO	MgO	SO <sub>3</sub>	K <sub>2</sub> O	TiO <sub>2</sub>	SrO	MnO
24.0	9.2	31.1	27.1	0.8	1.0	1.60	1.74	0.808	0.779

Geopolymer cement consisting of fly ash, NaOH, and Na<sub>2</sub>SiO<sub>3</sub> was ground in a ball mill. Sucrose was used as a superplasticizer to improve the workability of GPC. Ordinary Portland cement was used to prepare OPCC. Steel bars with 333 N/mm<sup>2</sup> yield strength and 6 mm diameter were used for fabricating spiral reinforcement cages with 114 mm diameter. The spiral pitches used were 50 mm (volumetric ratio of confining reinforcement 2.06%). GPC and PCC specimens are named GPC S50 and OPCC S50, which correspond to pitches of 50 mm respectively. GPC S0 and OPCC S0 are unconfined GPC and OPCC specimens. GPC mix was prepared according to the guidelines given in the literature [6], [13], while OPCC mix was also prepared according to SNI 2834:2000, and the details are given in Table 4.

Table 2. Coarse Aggregate Properties

Parameter	Measured value	Unit
Specific gravity	2.77	-
Moisture content	1.06	%
Absorption	1.63	%

Table 3. Fine Aggregate Properties

Parameter	Measured value	Unit
Specific gravity	2.73	-
Moisture content	6.50	%
Absorption	3.10	%

Table 4. Mix Proportions

Mix	Cement (kg/m <sup>3</sup> )	Fly Ash (kg/m <sup>3</sup> )	NaOH <sub>(s)</sub> (kg/m <sup>3</sup> )	Na <sub>2</sub> SiO <sub>3(s)</sub> (kg/m <sup>3</sup> )	Coarse Aggregate (kg/m <sup>3</sup> )	Fine Aggregate (kg/m <sup>3</sup> )	Water (kg/m <sup>3</sup> )	Superplasticizer (kg/m <sup>3</sup> )
GPC	-	596.7	36.1	55.5	1141.4	496.3	147.1	5.97
OPCC	410.0	-	-	-	1137.5	636.9	211.5	-

## 2.2. Preparation of Test Specimens

The manufacture of specimens using dry method [6]. The mixing sequence is shown in Figure 1. Coarse and fine aggregate in saturated dry surface condition were first mixed in a concrete mixer for about three minutes. Geopolymer cement and superplasticizer were added and mixed for five minutes. Then, water was added to the dry ingredients and mixed for ten minutes. GPC resembles OPCC in its appearance. Immediately after mixing, the slump of fresh concrete was measured to observe the consistency of the mixture. Cylinders of 100 mm diameter and 200 mm height were prepared to determine the compressive strength, modulus of elasticity, and splitting tensile strength respectively. To find the stress-strain behavior, cast iron molds of 150 mm diameter and 300 mm height were made. After casting, GPC specimens were kept at room temperature for 28 days. Under laboratory environmental conditions, the test specimens were left until the day of testing. OPCC specimens were also prepared and kept in water for 28 days after one day of casting. Three GPC specimens and three OPCC specimens were cast for each confinement pitch.

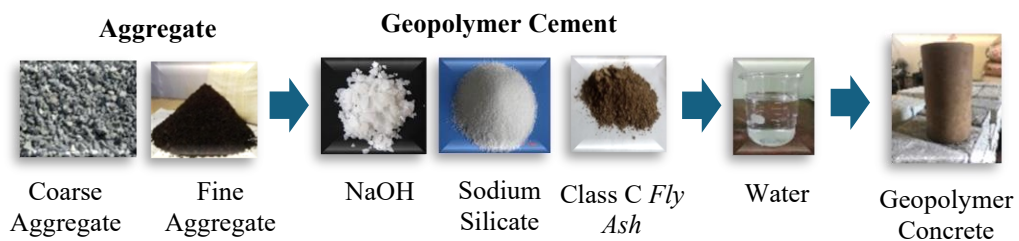


Figure 1. Sequence in Mixing

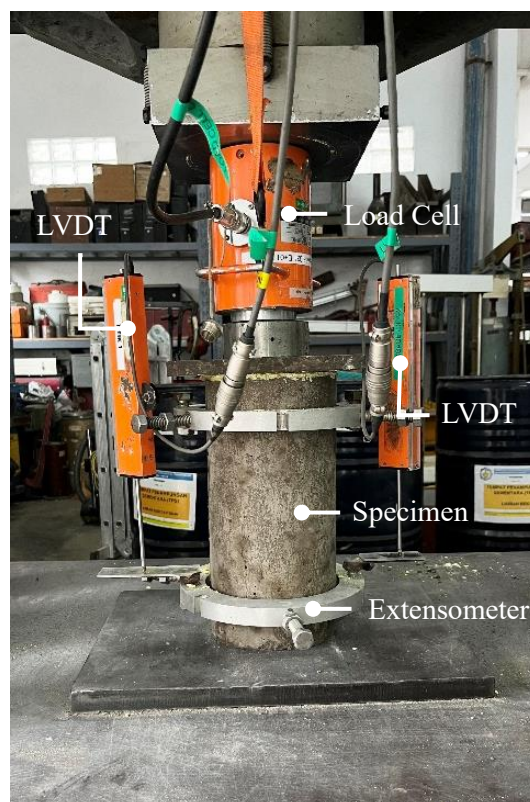


Figure 2. Loading Arrangement

## 2.3. Testing

The specimens were tested for compressive strength, modulus of elasticity, and splitting tensile strength 28 days after casting. The stress-strain behaviors were determined by performing tests on cylindrical specimens. The LVDTs with the lowest count of 0.01 mm were used. The specimens were placed in a compression testing machine (2000 kN

capacity) and tested under uniaxial compression. The LVDTs were attached to the extensometer and were parallel to the longitudinal axis. The loading arrangement is shown in Figure 2.

### 3. Results and Discussion

#### 3.1. Fresh and Hardened Properties

The slump testing results, compressive strength, elastic modulus, and splitting tensile strength are presented in Table 5. The slump value of geopolymer concrete was obtained at 200 mm as shown in Figure 3. This result showed good workability. Previous study [9] found that the slump results of fresh geopolymer concrete using sucrose was 165-195 mm. For mixes with high NaOH content (S:H = 1), the setting setting was controlled by normal geopolymerization [15]. At low NaOH concentrations, the dissolution of  $Si^{4+}$  and  $Al^{3+}$  ions in fly ash decreased [16], which reduced geopolymerization and thus increased the setting time, thus the workability of fresh concrete to be higher. It can be observed that GPC mix design produced concrete compressive strength that was close to the high strength classification according to ACI 318, while the OPCC mix design produced normal strength.



Figure 3. Slump Test

Table 5. Fresh and hardened properties of GPC and OPCC mixtures

Mix	Slump (mm)	Compressive Strength (MPa)	Splitting Tensile Strength (MPa)	Splitting Tensile Strength to Compressive Strength Ratio
GPC	200	39.43	4.24	0.108
OPCC	160	27.34	3.63	0.132

The calcium content in fly ash significantly affected the hardening of the geopolymer system [17]. A previous study [18] reported that the strength of fly ash-based geopolymer concrete is related to the reaction products with the addition of C-S-H and C-A-S-H gels together with N-A-S-H gels. The NaOH concentration affects the dissolution of silica and alumina, and the release of calcium from fly ash [3]. The release of  $Si^{4+}$  and  $Al^{3+}$  ions from fly ash particles according to NaOH concentration also affects their strength due to the formation of N-A-S-H gels, which increase geopolymerization [16]. In addition, the ratio of  $Na_2SiO_3$  to NaOH (S:H) also affects the strength of class C fly ash-based geopolymer concrete [4].

Table 6. Elastic Modulus ( $E_c$ ) of GPC and OPC Concrete

Mix	Elastic Modulus (MPa)		$\frac{E_c \text{ Experiment}}{E_c \text{ ACI 318}}$
	Experiment	ACI 318	
GPC	26726	33374	0.80
OPCC	21320	25614	0.83

The ratio of splitting tensile strength to compressive strength was 10.8% and 14.2% for GPC and OPCC, respectively. A study on class C fly ash-based geopolymer concrete by [4] with a NaOH molarity of 10–15 M obtained splitting tensile strength to compressive strength ratio of 8.2–10.5%. The results of this study produced a splitting tensile strength to compressive strength ratio that was close to the results of previous studies.

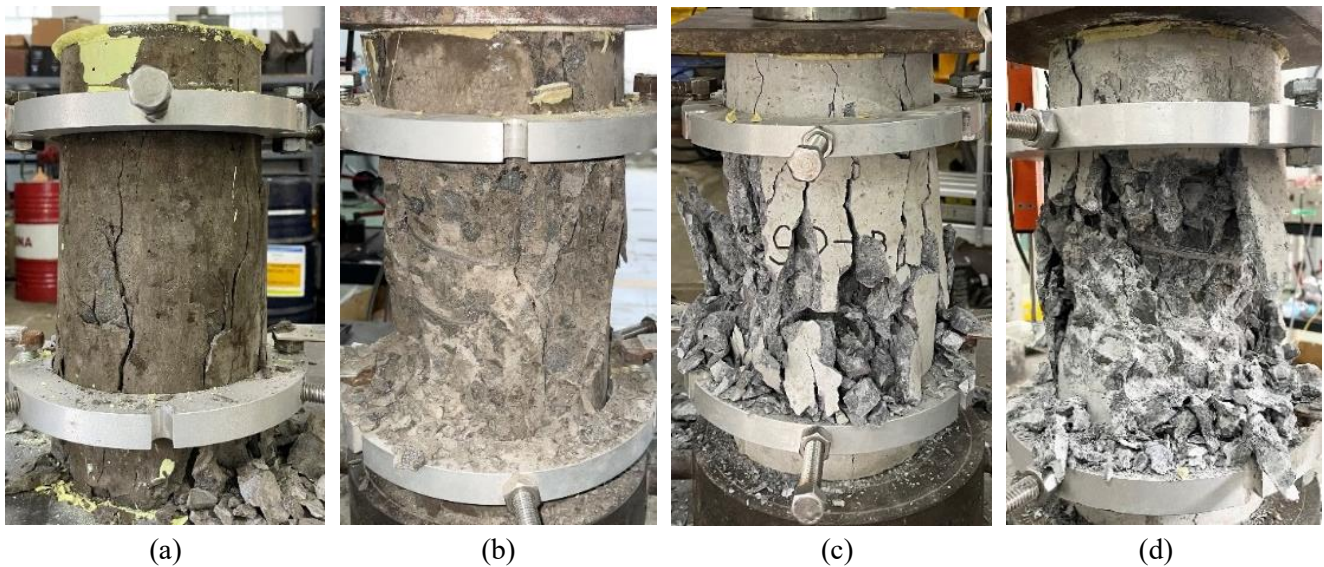


Figure 4. Tested Specimens (a) GPC S0; (b) GPC S50; (c) OPC S0; (d) OPC S50

$$E_c = 0,043 w^{1,5} \sqrt{f'_c} \quad (1)$$

where  $w$  and  $f'_c$  are the density of concrete and unconfined concrete stress.

The elastic modulus of GPC and OPC concrete are presented in Table 6. Geopolymer concrete has an elastic modulus of 26.7 GPa for a compressive strength of around 39 MPa. This value was around 20% lower than the theoretical value estimated using ACI 318 (1). Research by [19] showed that the elastic modulus of geopolymer concrete was 11–16% lower than the value of the ACI 318 equation. Similar results were also recorded in previous research by [20]. In addition, OPC concrete for a compressive strength of around 27 MPa obtained 21.3 GPa, 17% lower than the theoretical value estimated by the ACI 318 equation.

### 3.2. Stress-Strain Behavior

#### 3.2.1. Behavior of Specimens

Figure 4 shows the failure of representative confined geopolymer and OPC concrete. Confined geopolymer and OPC concrete have failure patterns similar. In general, unconfined concrete (GPC S0) exhibits failure with sharp cracks. For confined concrete, the concrete cover was spalled along with vertical cracks on the sides of the specimen. In the case of geopolymer concrete specimens, confinement is exposed because of the large amount of spalled concrete cover. The core of concrete was found to be relatively more intact (GPC S50).

#### 3.2.2. Strength Enhancement

The enhancement strength is the ratio of the peak stress of the confined concrete to the peak stress of unconfined concrete [14], as shown in Table 7 for GPC, and for OPCC in Table 8. The strength enhances by 34% at spiral confinement volumetric ratios of 2.06% for geopolymer concrete and by 30% for OPC concrete. Strain enhancement is the ratio of strain at confined concrete peak stress to strain at unconfined concrete peak stress and is also a measure of ductility. This obtained an increase in strain of 2.66 for GPC and 2.60 for OPCC. This results in a significant increase in the strength and ductility of the concrete.

Table 7. Effect of Confinement on the Strength of GPC

Mix	Peak Stress	Strength Enhancement	Strain at Peak Stress	Strain Enhancement
GPC S0	39.43	1.00	0.0021	1.00
GPC S50	52.78	1.34	0.0055	2.66

Table 8. Effect of Confinement on the Strength of OPCC

Mix	Peak Stress	Strength Enhancement	Strain at Peak Stress	Strain Enhancement
OPC S0	27.34	1.00	0.0022	1.00
OPC S50	35.50	1.30	0.0056	2.60

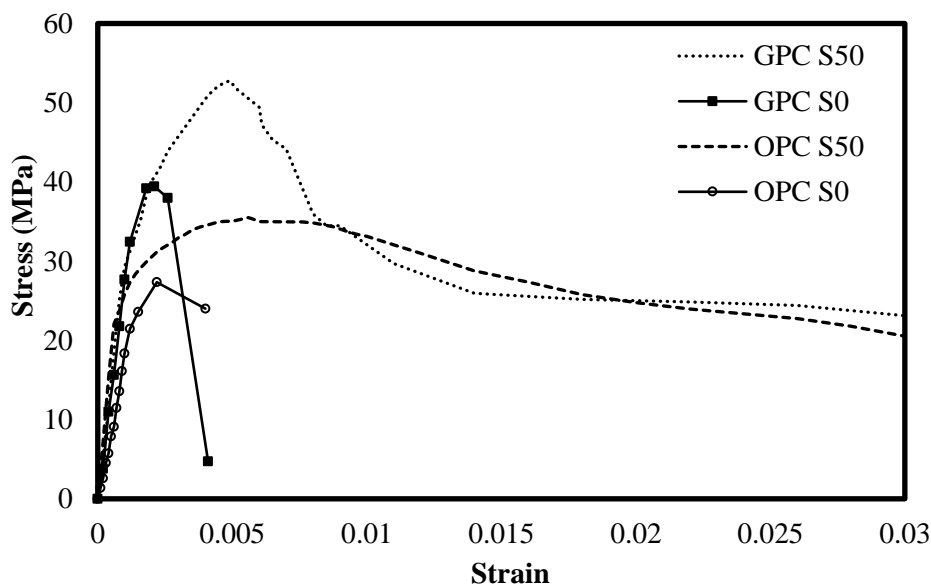


Figure 5. Stress-strain Curve of Confined GPC and OPC concrete

### 3.2.3. Stress-Strain Curve

The stress-strain curve of geopolymer concrete is shown in Figure 5. When geopolymer concrete is confined at a low stress level, and its transverse reinforcement is almost not stressed, so the concrete appears to be unconfined. Concrete will be confined at a stress approaching uniaxial strength [21]. This confinement greatly enhances the stress-strain characteristics of geopolymer concrete under increasing strain. The plain geopolymer concrete (GPC S0) specimens experienced brittle failure. This is consistent with the behavior of confined geopolymer concrete, which is relatively more brittle compared to the confined OPC concrete. The post-peak stress decrease was sharper in geopolymer concrete specimens. Confined OPC concrete showed better ductile behavior due to the lateral stress received from the confinement. The use of confinement significantly improved the stress-strain characteristics of geopolymer and OPC concrete at higher strain rates. The stress-strain behavior of geopolymer concrete was improved using confining reinforcement.

### 3.3. Evaluation of Ultimate Condition

This section investigates the application of the current models for models for OPC concrete to predict the ultimate conditions of confined geopolymer concrete. So far, many models based on the theoretical and experimental results have been proposed to evaluate ultimate conditions including ultimate stress and strain of normal-strength and high strength OPCC. The analytical model proposed by Richard et al. [22] was selected to evaluate the ultimate compressive strength and ultimate compressive strain of confined geopolymer concrete in this study. The equations of this model are listed in follows:

Richard et al. model [22]:

$$f_{cc} = f'_{co} + k_1 f_l \tag{2}$$

$$\varepsilon_{cc} = \varepsilon_{co} \left( 1 + k_2 \frac{f_l}{f'_{co}} \right) \tag{3}$$

where  $f_{cc}$  and  $\varepsilon_{cc}$  are the peak concrete stress and strain,  $f_l$  is lateral pressure,  $f'_{co}$  and  $\varepsilon_{co}$  are the unconfined concrete stress and strain,  $k_1$  and  $k_2$  are coefficients that are functions of the concrete mix and the lateral pressure. Richart et al. [22] proposed the average values of the coefficients  $k_1 = 4.1$  and  $k_2 = 5k_1$ . It also adopted the equations proposed by Popovics [23] to describe the entire stress–strain curve of confined concrete and is given below.

$$f_c = \frac{f_{cc} \left( \frac{\varepsilon_c}{\varepsilon_{cc}} \right)^r}{r - 1 + \left( \frac{\varepsilon_c}{\varepsilon_{cc}} \right)^r} \tag{4}$$

where,  $f_c$ ,  $\varepsilon_c$ ,  $r$ , are the stress at any point, strain at any point, and  $r$  is the curve fitting factor. The expression for ‘ $r$ ’ adopted equation proposed by Mander et al. [24] is given by (5),

$$r = \frac{E_c}{E_c + E_{sec}} \tag{5}$$

$$E_{sec} = \frac{f_{cc}}{\varepsilon_{cc}} \tag{6}$$

where  $E_c$  is the modulus of elasticity of concrete and the parameter  $E_{sec}$  is given by (6).

The comparisons of ultimate stress and strain of specimens between experimental and predicted results using Richard et al. model is shown in Table 9. As obviously indicated, Richard model underestimated the experimental results of ultimate stress and strain of confined geopolymer concrete. The values of the ratios of prediction to experiment of them were 0.92 and 0.78, respectively. Richard model has good results of ultimate stress and strain of confined OPC concrete. The values of the ratios of prediction to experiment of them were 1.04 and 0.93, respectively. Generally, Richard model underestimated both ultimate stresses and strains of confined geopolymer concrete. For OPC concrete, Richard model was predicted in good agreement with experimental results.

Table 9. Comparisons of Ultimate Conditions: (a) Confined Strength; (b) Confined Strain.

Specimens	Predicted to Experimental ( $f_{cc}/f_{co}$ ) Ratio	Predicted to Experimental ( $\varepsilon_{cc}/\varepsilon_{co}$ ) Ratio
GPC S50	0.92	0.78
OPC S50	1.04	0.93

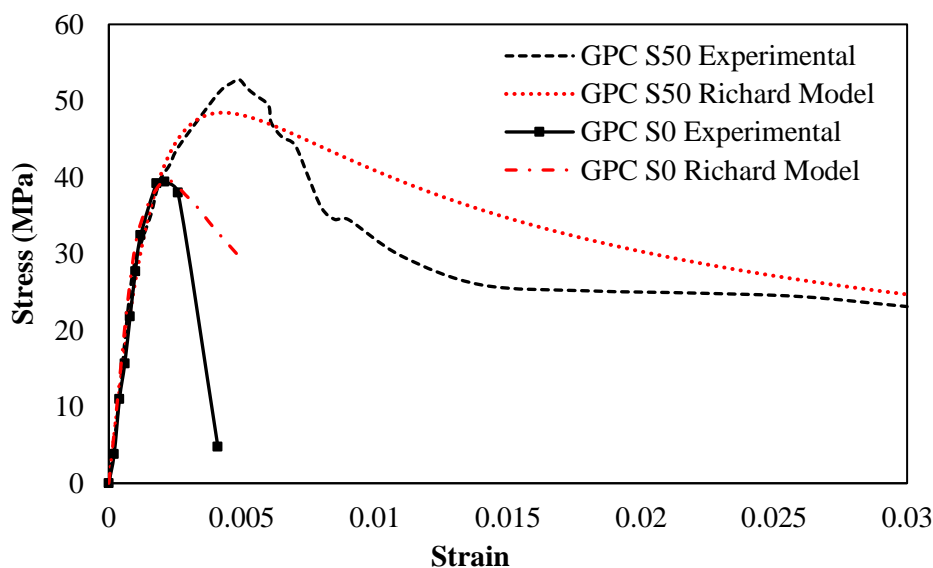


Figure 6. Stress-strain Curve of Confined Geopolymer Concrete between Predicted Results using Richard Model and Experimental Results

### 3.3.1. Evaluation of Axial Stress-Strain Curve

The axial stress-strain relationship of concrete is a basis to analyze the structural performances of structural components, it is necessary and important to understand the axial stress-strain behavior of confined geopolymer concrete. Figure 6 shows the comparisons of the axial stress-strain behaviors of confined and unconfined geopolymer concrete between predicted results using Richard model and experimental results. It was observed by inspection of these results that the Richard model has identical ascending branches of the stress-strain behavior of specimens. However, an interesting observation was that the Richard model underestimated the descent branches of confined and unconfined geopolymer concrete, therefore meaning that this model is not capable of predicting the stress-strain behavior well, more analytical analysis is needed to refine the accuracy of the constitutive model for confined geopolymer concrete. As indicated, the predicted results of the descending branches of confined and unconfined OPC concrete using the Richard model were reasonably in good agreement with the experimental results, shown in Figure 7.

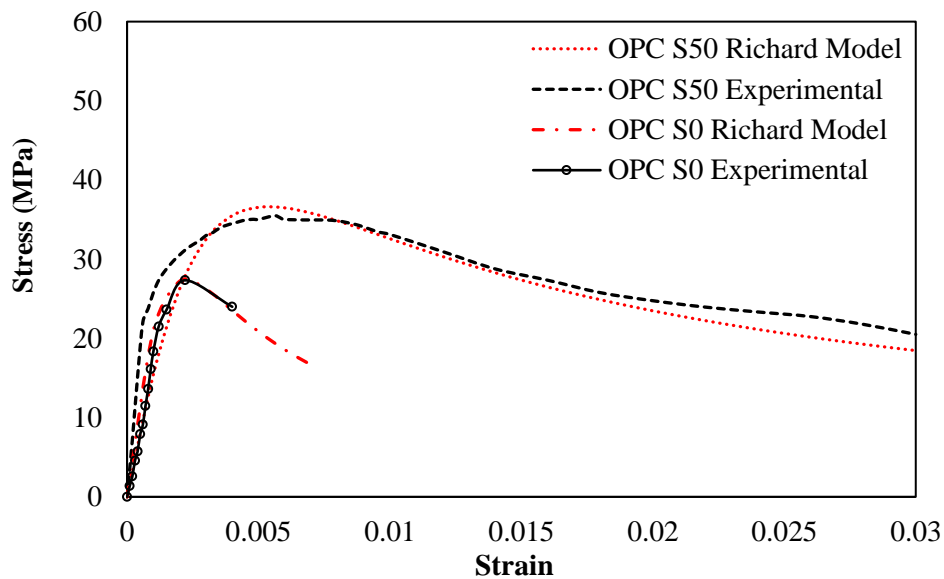


Figure 7. Stress-strain Curve of Confined OPC Concrete between Predicted Results using Richard Model and Experimental Results

## 4. Conclusions

Based on the obtained data in this experiment, the following conclusions can be made. The use of confinement enhanced the strength and ductility of the geopolymer concrete. The strength of geopolymer concrete at a spiral confinement volumetric ratio of 2.06% increased by 34% and by 30% for OPC concrete. Strain enhancement indicated an increase in the ductility of GPC and OPC concrete. The hardening phase of the stress-strain curves of geopolymer concrete and OPC concrete showed similar behavior, whereas the decrease in stress after peak stress (softening phase) was sharper in the geopolymer concrete. Richard model is not capable of predicting the stress-strain behavior for confined and unconfined geopolymer concrete, whereas, for OPC concrete, Richard model was predicted in good agreement with experimental results. More analytical analysis is needed to refine the accuracy of the constitutive model for confined geopolymer concrete.

## Acknowledgment

The author would like to acknowledge the financial support Beasiswa Pendidikan Indonesia (BPI) from Directorate General of Higher Education of the Ministry of Education and Culture of Republic of Indonesia (Kemendikbudristek RI) for sponsoring the author to study at Institut Teknologi Sepuluh Nopember, Surabaya, Indonesia.



## References

- [1] N. P. Rajamane, M. C. Nataraja, J. K. Dattatreya, N. Lakshmanan, and D. Sabitha, "Sulphate resistance and eco-friendliness of geopolymer concretes," *Indian Concr. J.*, vol. 86, no. 1, pp. 13–22, 2012.
- [2] J. Davidovits, "Properties of Geopolymer Cements," *First Int. Conf. Alkaline Cem. Concr.*, pp. 131–149, 1994.
- [3] S. Hanjitsuwan, S. Hunpratub, P. Thongbai, S. Maensiri, V. Sata, and P. Chindapasirt, "Effects of NaOH concentrations on physical and electrical properties of high calcium fly ash geopolymer paste," *Cem. Concr. Compos.*, vol. 45, pp. 9–14, 2014.
- [4] P. Topark-Ngarm, P. Chindapasirt, and V. Sata, "Setting Time, Strength, and Bond of High-Calcium Fly Ash Geopolymer Concrete," *J. Mater. Civ. Eng.*, vol. 27, no. 7, pp. 1–7, 2015.
- [5] Y. Tajunnisa, M. Sugimoto, T. Sato, and M. Shigeishi, "A study on factors affecting geopolymerization of low calcium fly ash," *Int. J. GEOMATE*, vol. 13, no. 36, pp. 100–107, 2017.
- [6] R. Bayuaji, A. K. Yasin, T. E. Susanto, and M. S. Darmawan, "A review in geopolymer binder with dry mixing method (geopolymer cement)," *AIP Conf. Proc.*, vol. 1887, no. July, 2017.
- [7] N. A. Husin, R. Bayuaji, Y. Tajunnisa, M. S. Darmawan, and P. Suprobo, "Performance of high calcium fly ash based geopolymer concrete in chloride environment," *Int. J. GEOMATE*, vol. 19, no. 74, pp. 107–113, 2020.
- [8] Y. N. Wibowo, B. Pisceca, and Y. Tajunnisa, "Numerical Investigation of Geopolymer Reinforced Concrete Beams Under Flexural Loading Using 3Dnlfea," *J. Civ. Eng.*, vol. 37, no. 1, p. 27, 2022.
- [9] N. A. Husin, "The Effect of Admixture Variations on Workability and Compressive Strength of Geopolymer Concrete Fly Ash Based With High Calcium Content," *Int. J. GEOMATE*, vol. 22, no. 92, pp. 116–123, 2022.
- [10] Y. Tajunnisa, N. A. Husin, S. Darmawan, R. Bayuaji, R. B. Darmawan, and A. A. Cahyani, "Performance of Workability and Compressive Strength on Self-Compacting Geopolymer Concrete Based On High-Calcium Fly Ash With Addictive Admixture," *IPTEK J. Eng.*, vol. 9, no. 1, p. 1, 2023.
- [11] M. S. Mansur, P. Suprobo, Y. Tajunnisa, and A. Kumala, "An Experiment of Shear Strength Reinforced Geopolymer Concrete Beam Based High-Calcium Fly Ash with Varian Shear Span-to-Depth Ratio," *J. Civ. Eng.*, vol. 38, no. 3, pp. 139–145, 2023.
- [12] Y. Tajunnisa, N. A. Husin, A. Kusbiantoro, A. Daffa Azmi, K. Fadilah Ashara, and M. Shigeishi, "Performance Changes in Mass and Compressive Strength of High-Calcium Fly Ash Based Geopolymer Concrete Due to Sodium Sulphate Exposure," *IPTEK J. Eng.*, vol. 10, no. 1, p. 1, 2024.
- [13] T. Phoo-Ngernkham, C. Phiangphimai, N. Damrongwiriyanupap, S. Hanjitsuwan, J. Thumrongvut, and P. Chindapasirt, "A Mix Design Procedure for Alkali-Activated High-Calcium Fly Ash Concrete Cured at Ambient Temperature," *Adv. Mater. Sci. Eng.*, vol. 2018, 2018.
- [14] N. Ganesan, R. Abraham, S. Deepa Raj, and D. Sasi, "Stress-strain behaviour of confined Geopolymer concrete," *Constr. Build. Mater.*, vol. 73, pp. 326–331, 2014.
- [15] P. Chindapasirt, P. De Silva, K. S. Crentsil, and S. Hanjitsuwan, "Effect of SiO<sub>2</sub> and Al<sub>2</sub>O<sub>3</sub> on the setting and hardening of high calcium fly ash-based geopolymer systems," *J. Mater. Sci.*, vol. 47, no. 12, pp. 4876–4883, 2012.

- [16] U. Rattanasak and P. Chindaprasirt, "Influence of NaOH solution on the synthesis of fly ash geopolymer," *Miner. Eng.*, vol. 22, no. 12, pp. 1073–1078, 2009.
- [17] S. Pangdaeng, T. P. Ngerkham, V. Sata, and P. Chindaprasirt, "Influence of curing conditions on properties of high calcium fly ash geopolymer containing Portland cement as additive," *Mater. Des.*, vol. 53, pp. 269–274, 2014.
- [18] A. Palomo, A. F. Jiménez, G. Kovalchuk, L. M. Ordoñez, and M. C. Naranjo, "Opc-fly ash cementitious systems: Study of gel binders produced during alkaline hydration," *J. Mater. Sci.*, vol. 42, no. 9, pp. 2958–2966, 2007.
- [19] J. R. Yost, A. Radlińska, S. Ernst, and M. Salera, "Structural behavior of alkali activated fly ash concrete. Part .Mixture design, material properties and sample fabrication," *Mater. Struct. Constr.*, vol. 46, no. 3, pp. 435–447, 2013.
- [20] D. Hardjito and B. V Rangan, "Development and Properties of Low-calcium Fly Ash Based Geopolymer Low-Calcium Fly Ash-Based Geopolymer Concrete By Faculty of Engineering Curtin University of Technology," *Aust. Univ. Technol. Perth*, no. January, p. 48, 2005.
- [21] R. Park and T. Paulay, "Reinforced Concrete Structures - Park\_Paulay." pp. 1–783, 1975.
- [22] R. L. Richart, F. Erwin, Brandtzaeg, Anton, and Brown, "A study of the failure of concrete under combined compressive stresses," *Univ. Illinois. Eng. Exp. Station. Bull.*, vol. 26, p. 12, 1928.
- [23] S. Popovics, "A Numerical Approach To The Complete Stress-Strain Curve of Concrete," *Cem. Concr. Res.*, vol. 3, no. 5, pp. 583–599, 1973.
- [24] J. B. Mander, M. J. N. Priestley, and R. Park, "Theoretical Strss-Strain Model for Confined Concrete," *J. Struct. Eng*, vol. 114, no. 8, pp. 1804–1826, 1988.